Random-coincidence corrections using iterative reconstruction for PET images

Jyh-Cheng Chen[a], Ren-Shyan Liu[b], Kao-Yin Tu[a], Henry Horng-Shing Lu*[c], Tai-Been Chen[c], and Kuo-Liang Chou[b]

[a]Institute of Radiological Sciences, National Yang-Ming University, Taipei, 112, Taiwan
[b]National PET/Cyclotron Center, Taipei Veterans General Hospital, Taipei, 112, Taiwan
[c]Institute of Statistics, National Chiao Tung University, Hsinchu, 30050, Taiwan

ABSTRACT

Iterative reconstruction (IR) algorithms can reduce artifacts caused by filtered backprojection (FBP) or convolution backprojection (CBP). Recently, the computational effects required for IR of positron emission tomography (PET) studies have been reduced to make it practically appealing. We have made an implementation of the improved Maximum Likelihood-Expectation Maximization (ML-EM) algorithm. The transition matrix was generated based on the geometry of the instrument. Phantoms of 6 line sources and 19 line sources were used to test our accelerated ML-EM algorithms against the FBP method. The singles were used to calculate the random coincidence rates by a well known formula and were compared to the randoms obtained by another geometric method. We also designed a new model using two line sources to determine the ratio of random events to true events. The artifacts near those line sources were eliminated with the ML-EM method. With decay correction, the RC events were uniformly distributed in whole field after 10 iterations. The ML-EM reconstructed images are superior to those obtained with FBP. The patterns of randoms provide insightful information for random correction, which the hardware correction by the delay window can not provide. This information is particular valuable when the delay window correction is not available in the old fashion PET scanner.

Keywords: Random coincidence, true coincidence, positron emission tomography, iterative reconstruction

1. INTRODUCTION

Nuclear medicine imaging diagnosis not only can detect functional and metabolic abnormality but also can do quantitative studies, thus it becomes an important clinical diagnostic modality. Recently there is a trend using PET for metabolic and physiological studies, for example glucose metabolic rate in the brain. In doing so, we need to generate accurate parametric[1]

* Correspondence: Email: rsliu@npcc.gov.tw; Tel: 886-2-28715849; Fax: 886-2-28749431

Penetrating Radiation Systems and Applications II, F. Patrick Doty, H. Bradford Barber, Hans Roehrig, Edward J. Morton, Editors, Proceedings of SPIE Vol. 4142 (2000) © 2000 SPIE. · 0277-786X/00/$15.00

images. In order to get such accurate images for quantitative analysis, we need to use better image reconstruction algorithms. Many commercial PET systems use the CBP technique for image reconstruction due to its fast computational speed. However, this method has several drawbacks. First, it is derived from the transmission tomography, not the emission tomography. It is therefore incapable of handling accidental coincidence (AC) or random coincidence (RC) events and attenuation that occur frequently in practice. Second, it does not consider the random variations that are inherent of the photon counts of coincidence events. Hence, the reconstructed images are typical noisy and inaccurate. Therefore, it is necessary to consider a realistic model for PET with RC events and attenuation. Based on this model, reconstruction methods with regularization are important to reduce the noise and edge artifact. Due to fast progress of computer technology, computers with very fast computing speeds are developed. Thus, using iterative reconstruction algorithms for such as ML-EM[1], in clinical setting have been reported recently. This paper describes our work on RC correction using ML-EM and shows some comparisons with CBP reconstructed images.

2. MATERIALS AND METHODS

The principle of PET is based on annihilation coincidence detection and tomographic images are formed through reconstruction step[2]. The PET scanner is Scanditronix PC4096-15WB whole-body scanner[3]. A total of 4096 crystals are arranged in eight rings of 512 crystals each. Two dual photomultiplier tubes (PMTs) are mounted on each assembly of 16 crystals. Transaxial field of view (FOV) is 55 cm and axial FOV is 9.75 cm. We used Ga68 that were produced by Ge68 – Ga68 generator with a half-life of 68 min[4]. In order to understand the detection, performance characteristics and data format, we designed the following experiments: 1. Phantom of two line sources separated by 2 cm were located at the central field of view (FOV) with a FOV of 26 cm, sinograms were obtained from a 10 min data acquisition. 2. Phantom of six line sources were located unevenly (intervals between line sources are 1, 3, 5, 5, and 4 cm, respectively), FOV was set to be 55 cm, acquisition time is 10 min. 3. Phantom of two line sources with equal activity (1:1) were separated by 13 cm. They were imaged at the same time for 10 min, then one line source was removed to image the other and vice versa. 4. Activity ratios were changed to be (3:1), (3:2), and (2:1), respectively, and step 3 was repeated again. 5. Two point sources separated by 2 cm were located at the central FOV with a 10 min scan.

2.1. The ML-EM Algorithm

According to the configuration of V.G.H.-Taipei PET system, the target image is partitioned into B=128*128 boxes (pixels) and there are D=256*193 detector tubes recorded in a sinogram of a slice. The intensity at each box, denoted by $\lambda(b), \quad b = 1,2,\cdots,B$, represents the average intensity within the corresponding box. The number of coincidence events recorded in each detector pair is denoted by $n^*(d), d = 1,2,...,D$. The statistical model (in incomplete space) is assumed to be

$$n^*(d) \text{ i.n.i.d. } Poisson(\lambda^*(d)), \tag{1}$$

where

$$\lambda^*(d) = \sum_{b=1}^{B} p(b,d)\lambda(b). \tag{2}$$

Here "i.n.i.d." means "independently and not identically distributed as," $\lambda^*(d)$ is the average intensities of coincident events at detector tube d, $p(b,d)$ is the transition probability from box b to detector tube d that may include in attenuation correction (Shepp and Vardi[1], Vardi, Shepp, and Kaufman[5]). For the purpose of applying the EM algorithm, one can assume the complete space model as

$$n(b,d) \text{ i.n.i.d. } Poisson(p(b,d)\lambda(b)). \tag{3}$$

The MLE-EM algorithm is derived as follows. The log-likelihood function in incomplete data space is

$$l(\lambda) = \sum_{d=1}^{D}\{\sum_{b=1}^{B} n^*(d)\ln[\lambda^*(d)] - \lambda^*(d)\} + \text{constant} \quad . \tag{4}$$

In contrast, the log-likelihood function in the above complete data space is

$$l_c(\lambda) = \sum_{d=1}^{D}\sum_{b=1}^{B}\{n(b,d)\ln[P(b,d)\lambda(b)] - p(b,d)\lambda(b)\} + constant \quad . \tag{5}$$

The E-step needs to compute the conditional expectation of the complete space log-likelihood. It is

$$Q = E\{l_c(\lambda \mid n^*, \lambda^{*old})\} = \sum_{d=1}^{D}\sum_{b=1}^{B}\{n^*(d)\frac{p(b,d)\lambda^{old}(b)}{\lambda^{*old}(d)}\ln[p(b,d)\lambda(b)] - p(b,d)\lambda(b)\} + constant \ , \tag{6}$$

where

$$\lambda^{*old}(d) = \sum_{b=1}^{B} p(b,d)\lambda^{old}(b). \tag{7}$$

The M-step requires the maximization of the conditional expectation in the E-step. This can be achieved by letting

$$\frac{\partial Q}{\partial \lambda(b)} = 0, b = 1,2,\cdots,B. \tag{8}$$

That is,

$$\frac{\partial Q}{\partial \lambda(b)} = \sum_{d=1}^{D}\{n^*(d)\frac{p(b,d)\lambda^{old}(b)}{\lambda^{*old}(d)}\frac{1}{\lambda(b)} - p(b,d)\} = 0. \tag{9}$$

Hence, the updating formula is

$$\lambda^{new}(b) = \frac{\lambda^{old}(b)}{p(b,\cdot)}\sum_{d=1}^{D} n^*(d)\frac{p(b,d)}{\lambda^{*old}(d)}, \tag{10}$$

where

$$p(b,\cdot) = \sum_{d=1}^{D} p(b,d). \tag{11}$$

In summary, the MLE-EM algorithm for PET is as follows.

•Algorithm 1. The EM Algorithm for PET:

Step 1. Initial: $\lambda^{old}(b), \quad b = 1,2,\cdots,B$ is obtained by the method of moments estimate (MME), the convolution backprojection (CBP) method, or other methods.

Step 2. Project: $\lambda^{*old}(d) = \sum_{b=1}^{B} p(b,d)\lambda^{old}(b)$ for d=1,…,D.

Step 3. Backproject: for b=1, 2, …, B,

$$\lambda^{new}(b) = \frac{\lambda^{old}(b)}{p(b,\cdot)} \sum_{d=1}^{D} n^*(d) \frac{p(b,d)}{\lambda^{*old}(d)}.$$

Step 4. Stop: If $l(\lambda^{new}) - l(\lambda^{old}) < tol$, for a tolerance level,

then stop. Else, $\lambda^{old}(b) \leftarrow \lambda^{new}(b)$, and go to Step 2.

2.2. The ML-EM Algorithm for Detecting Random Coincidence Events

A new model for these three sinograms by considering decay correction is proposed as follows. Suppose

$$n_i^*(d) \text{ i.n.i.d. } Poisson(c_i \lambda_i^*(d)), i = 1,2,3, d = 1,2,\cdots,D, \tag{12}$$

where $n_i^*(d)$, i = 1, 2, 3, are mutually independent,

$$\lambda_i^*(d) = \sum_{b=1}^{B} p(b,d)\lambda_i(b), i = 1,2, \tag{13}$$

$$\lambda_3^*(d) = \sum_{b=1}^{B} p(b,d)(\lambda_3(b) + \lambda_{RC}(b)), \quad \lambda_{RC}(b) \geqq 0, \tag{14}$$

and

$$\lambda_3(b) = \lambda_1(b) + \lambda_2(b). \tag{15}$$

For example, the half-life of Ga^{68} radionuclide is 68 minutes and the exponentially decay rate is $k = \frac{\ln 2}{68}$. Therefore, the decay factors for three sinograms are

$$c_i = e^{-kt_i}(1 - e^{-kt_i})/(kt_i), i = 1,2,3. \tag{16}$$

The log-likelihood function in the above incomplete data space is

$$l(\lambda_1,\lambda_2,k)=\sum_{d=1}^{D}\sum_{j=1}^{3}\{n_j^*(d)\ln[c_j\lambda_j^*(d)]-c_j\lambda_j^*(d)\}+\text{constant}. \tag{17}$$

The MLE-EM algorithm for this new model can be derived as follows. Suppose the complete data space is

$$n_i(b,d)\ \text{ i.n.i.d. }\ Poisson\ (c_i p(b,d)\lambda_i(b)), i=1,2, \tag{18}$$

$$n_3(b,d)\ \text{ i.n.i.d. }\ Poisson\ (c_3 p(b,d)(\lambda_3(b)+\lambda_{RC}(b))), \tag{19}$$

for $b=1,2,\cdots,B, d=1,2,\cdots,D$ and $n_i(b,d)$, i = 1, 2, 3, are mutually independent. Then the log-likelihood function in complete data space becomes

$$\begin{aligned} l_c(\lambda_1,\lambda_2,k)=&\sum_{d=1}^{D}\sum_{b=1}^{B}\{\sum_{j=1}^{2}n_j(b,d)\ln[c_j p(b,d)\lambda_j(b)]\\ &+n_3(b,d)\ln[c_3 p(b,d)(\lambda_3(b)+\lambda_{RC}(b))]\\ &-p(b,d)[c_1\lambda_1(b)+c_2\lambda_2(b)]\\ &-c_3 p(b,d)[\lambda_3(b)+\lambda_{RC}(b)]\}\\ &+constant\ . \end{aligned} \tag{20}$$

The E-step computes the conditional expectation:

$$\begin{aligned} Q=&E\{l_c(\lambda_1,\lambda_2,\lambda_{RC})\big|n_i^*,\lambda_i^{*old},i=1,2,3)\}\\ =&\sum_{d=1}^{D}\sum_{b=1}^{B}\{\sum_{j=1}^{2}n_j^*(d)\frac{p(b,d)\lambda_j^{old}(b)}{\lambda_j^{*old}(d)}\ln[c_j p(b,d)\lambda_j(b)]\\ &+n_3^*(d)\frac{p(b,d)(\lambda_3^{old}(b)+\lambda_{RC}^{old}(b))}{\lambda_3^{*old}(d)}\ln[c_3 p(b,d)(\lambda_3(b)+\lambda_{RC}(b))]\\ &-p(b,d)[c_1\lambda_1(b)+c_2\lambda_2(b)]\\ &-c_3 p(b,d)(\lambda_3(b)+\lambda_{RC}(b))\}+constant, \end{aligned} \tag{21}$$

where

$$\lambda_j^{*old}(d)=\sum_{b=1}^{B}p(b,d)\lambda_j^{old}(b), j=1,2, \tag{22}$$

$$\lambda_3^{*old}(d)=\sum_{b=1}^{B}p(b,d)(\lambda_3^{old}(b)+\lambda_{RC}^{old}(b)), \tag{23}$$

and

$$\lambda_3^{old}(b)=\lambda_1^{old}(b)+\lambda_2^{old}(b). \tag{24}$$

The M-step needs to maximize the conditional expectation in the E-step. This can be achieved by solving $\frac{\partial Q}{\partial \lambda_j(b)} = 0, \frac{\partial Q}{\partial \lambda_{RC}(b)} = 0$, for all $j = 1,2, b = 1,2,\cdots,B$. Since

$$\frac{\partial Q}{\partial \lambda_j(b)} = \sum_{d=1}^{D} \{ n_j^*(d) \frac{p(b,d)\lambda_j^{old}(b)}{\lambda_j^{*old}(d)} \frac{1}{\lambda_j(b)}$$

$$+ n_3^*(d) \frac{p(b,d)(\lambda_3^{old}(b) + \lambda_{RC}^{old}(b))}{\lambda_3^{*old}(d)} \frac{1}{\lambda_3(b) + \lambda_{RC}(b)}$$

$$- c_j p(b,d) - c_3 P(b,d) \} = 0, j = 1,2, \tag{25}$$

and

$$\frac{\partial Q}{\partial \lambda_{RC}(b)} = \sum_{d=1}^{D} \{ n_3^*(d) \frac{p(b,d)(\lambda_3^{old}(b) + \lambda_{RC}^{old}(b))}{\lambda_3^{*old}(d)} \frac{1}{\lambda_3(b) + \lambda_{RC}(b)}$$

$$- c_3 p(b,d) \} = 0. \tag{26}$$

Let

$$A_j(b) = \frac{\lambda_j^{old}(b)}{p(b,.)} \sum_{d=1}^{D} n_j^*(d) \frac{p(b,d)}{\lambda_j^{*old}(d)}, j = 1,2, \tag{27}$$

and

$$A_3(b) = \frac{\lambda_3^{old}(b) + \lambda_{RC}^{old}(b)}{p(b,.)} \sum_{d=1}^{D} n_3^*(d) \frac{p(b,d)}{\lambda_3^{*old}(d)}. \tag{28}$$

Then the above equations (25) and (26) become

$$\frac{A_1(b)}{\lambda_1(b)} + \frac{A_3(b)}{\lambda_1(b) + \lambda_2(b) + \lambda_{RC}(b)} = c_1 + c_3, \tag{29}$$

$$\frac{A_2(b)}{\lambda_2(b)} + \frac{A_3(b)}{\lambda_1(b) + \lambda_2(b) + \lambda_{RC}(b)} = c_2 + c_3, \tag{30}$$

and

$$\frac{A_3(b)}{\lambda_1(b) + \lambda_2(b) + \lambda_{RC}(b)} = c_3. \tag{31}$$

In order to maximize the conditional expectation Q and maintain the nonnegativeness of the new estimates, the following generalized EM (GEM) algorithm is considered.

• Algorithm 2. The GEM Algorithm for detecting RC events:

Step 1. Initial:

$\lambda_j^{old}(b)$ for $b = 1,2,\cdots,B$ by the MME, CBP, or other methods.

$$\lambda_{RC}^{old}(b) = 0.$$

Step 2. Project: $\lambda_j^{*old}(d)$ for $d = 1,2,\cdots,D$ by (13), (14), (15).

Step 3. Backproject:

$A_j(b)$ by (27), (28).

$$\lambda_1^{new}(b) \longleftarrow \frac{A_1(b)}{c_1},$$

$$\lambda_2^{new}(b) \longleftarrow \frac{A_2(b)}{c_2},$$

$$\lambda_3^{new}(b) \longleftarrow \lambda_1^{new}(b) + \lambda_2^{new}(b),$$

$$\lambda_{RC}^{new}(b) \longleftarrow \max\{(\frac{A_3}{c_3} - \frac{A_1}{c_1} - \frac{A_2}{c_2}), 0\}.$$

Step 4. Stop:

If $l(\lambda_j^{new}, \lambda_{RC}^{new}, j = 1,2) - l(\lambda_j^{old}, \lambda_{RC}^{old}, j = 1,2) < tol$ for a tolerance level, then stop. Else,

$\lambda_j^{old}(b) \leftarrow \lambda_j^{new}(b), \lambda_{RC}^{old}(b) \leftarrow \lambda_{RC}^{new}(b), j = 1,2$, and go to step2.

2.3. Random Coincidence Event Rate

The single rays were used to calculate the random coincidence event rates by the formula: $R_{AC} = 2\tau R_i R_j$ whereτ is the coincidence resolving time of the detectors and associated electronics, and R_i or R_j is the single-channel[6], i.e., the noncoincidence count rate in detector i or j. These RC rates were calculated using the raw data from the sinograms and were compared to the results obtained by geometric method. The geometric method uses the following formula:

$$R_S = 2E * \varepsilon * g * \exp(-\mu D/2)$$
$$R_T = \sum E * \varepsilon^2 * g * \exp(-\mu D)$$
$$R_{AC} = \sum 2 * \tau * R_s^2$$

where E is the source emission rate (positron/sec), ε is the intrinsic efficiency of a detector pair (assumed to be equal), i.e., fraction of incident photons detected, and g is the geometric efficiency of an individual detector, i.e., fraction of emitted photons intercepted by the detector[6]. D is the object thickness and μ is the linear attenuation coefficient of the object.

3. RESULTS AND DISCUSSION

1. From each raw projection data of the line source we get the corresponding sinogram. 2. From the line source sinogram we estimate the transition matrix for our EM reconstruction[7], and the reconstructed images were compared to the ones by FBP. The streak artifacts near those line sources seen on the FBP reconstructed images were completely eliminated with the ML-EM method (Fig 1). 3. On the spatial resolution comparisons: in the case of a FOV of 55 cm, FWHM is 9.66 mm from the FBP results as compared to 7.14 mm from the ML-EM results. In the case of a FOV of 26 cm, FWHM is 6.76 mm from the FBP results as compared to 5.81 mm from the ML-EM results (Fig. 2). 4. We also designed experiments using two line sources to study random coincidence distribution. A new model was proposed for our modified ML-EM algorithm for these types of experiments. With decay correction, the random coincidence events were uniformly distributed in whole field after 10 iterations[8,9], which becomes an important factor that causes error in quantification (Fig. 3 shows four different activity ratios between the two line sources). 5. With our modified ML-EM algorithm, we actually were able to reconstruct true and random coincidence events separately at the same time (Fig. 4). 6. We also used two point sources to determine the ratio of random coincidence events to true coincidence events. Using single rays, the numbers of random coincidence were calculated from the above mentioned formula. The numbers of true coincidence were obtained by subtracting corresponding randoms from total measured coincidence events. The random/true ratio was 47.05% to 78.23%, while in the geometric method, the random/true coincidence ratio was 33.87% to 59.61% (Table 1).

4. CONCLUSIONS

The ML-EM reconstructed images are superior to those obtained with FBP in terms of spatial resolution, artifacts and noise. The random/true ratios are high, which demonstrates the need for random correction. The patterns of random coincidence events provide insightful information for random correction, which the hardware correction by the delay window can not provide. This information is particular valuable when the delay window correction is not available as in the case of old fashioned PET scanners. With our modified ML-EM method, we are able to reconstruct the true and random coincidence events separately at the same time in the case of two line sources. In random coincidence studies, the results obtained by geometric method were close to the results calculated from experimental data, which verifies the random coincidence rate formula.

REFERENCES

1. L A. Shepp and Y. Vardi, "Maximum likelihood reconstruction for emission tomography," *IEEE Trans. Med. Imaging* **1**, pp. 113-122, 1982.

2. Spinks TJ, Jones T, Gilardi MC, Heather JD. Physical performance of the latest generation of commercial positron scanner," *IEEE trans. Nucl. Sci.* **35**, pp. 721-725, 1988.

3. SCANDITRONIX PC-4096-15WB Whole body PET scanner Service Menu.

4. G. B. Saha, *Fundamentals of Nuclear Pharmacy*, 1998.

5. Y. Vardi, L. A. Shepp, and L. Kaufman, ``A statistical model for positron emission tomography," *Journal of the American Statistical Association.* **80**, pp. 8-20, 1985.

6. J. A. Sorenson and M. E. Phelps, *Physics in Nuclear Medicine*, 2nd ed. Saunders, Philadelphia, 1987.

7. K. Lange and R. Carson, "EM reconstruction algorithms for emission and transmission tomography," *J. Comput. Assist. Tomogr.* **8**, pp. 306-316, 1984.

8. H. H.-S. Lu, C.-M. Chen, and I.-H. Yang, "Cross-reference weighted least square estimates for positron emission tomography," *IEEE Trans. Med. Imaging.* **17**, pp. 1-8, 1998.

9. H. H.-S. Lu and W.-J. Tseng, "On accelerated cross-reference maximum likelihood estimates for positron emission tomography," *IEEE Nuclear Science Symposium* **2**, pp. 1484-1488, 1997.

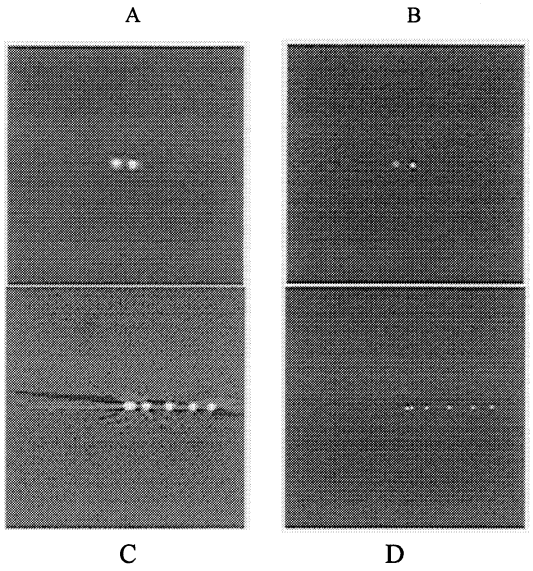

Figure 1: A: one slice of two line sources reconstructed by FBP, B: the same slice of two line sources reconstructed by ML-EM, C: one slice of six line sources reconstructed by FBP, D: the same slice of six line sources reconstructed by ML-EM.

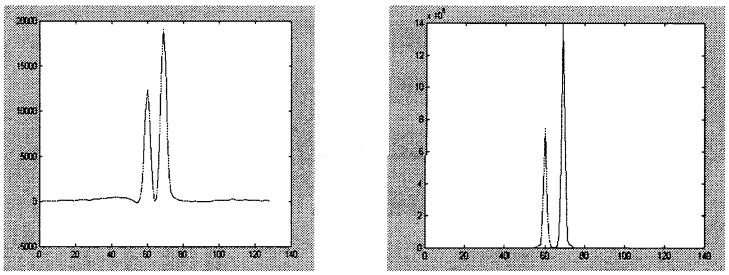

Figure 2: The horizontal trace of each of the four images shown in Fig. 1, respectively.

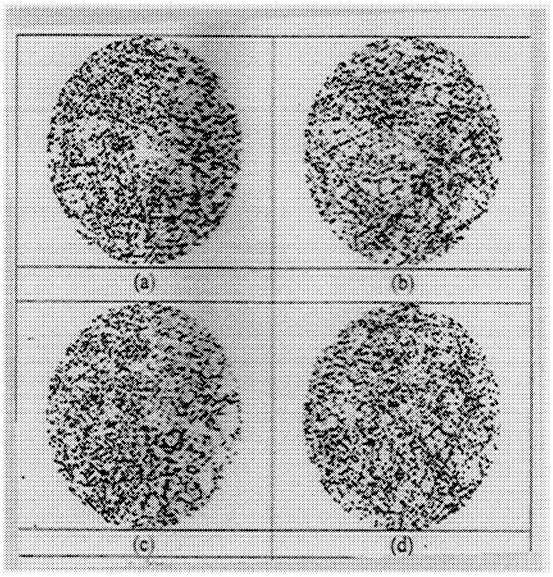

Figure 3: One slice of reconstructed random coincidence events from the two line sources using our modified ML-EM.

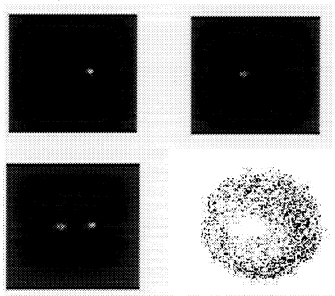

Figure 4: Using two line sources for random correction, upper two reconstructed images correspond to each of the line source acquired separately, the lower left is the reconstructed truce coincidence image corresponding to the two line sources acquired simultaneously, lower right is the corresponding reconstructed random coincidence image.

Table 1. Two point sources random coincidence studies with different activities using geometric and experimental methods, respectively.

		geometr				experim		
uCi	random	true	total	R/T	random	true	total	R/T
57.03	3.76E+08	6.31E+08	1.01E+09	59.61%	3.88E+08	4.96E+08	8.84E+08	78.23%
53.55	3.32E+08	5.93E+08	9.25E+08	55.99%	3.43E+08	4.85E+08	8.29E+08	70.68%
50.28	2.99E+08	5.56E+08	8.55E+08	53.80%	3.04E+08	4.75E+08	7.78E+08	63.99%
44.37	2.28E+08	4.91E+08	7.18E+08	46.38%	2.67E+08	4.64E+08	7.30E+08	57.50%
34.45	1.37E+08	3.81E+08	5.19E+08	36.05%	2.35E+08	4.48E+08	6.83E+08	52.34%
32.35	1.21E+08	3.58E+08	4.79E+08	33.87%	2.04E+08	4.34E+08	6.39E+08	47.05%